ISSN (Print) : 0974-6846
ISSN (Online) : 0974-5645

INDIAN JOURNAL OF SCIENCE AND TECHNOLOGY
January 2020, Vol 13(03), 277 – 285
DOI: 10.17485/ijst/2020/v13i03/149476,

Controlled Hydrothermal Synthesis of Nano-MoO_2 as Anode for Lithium Ion Battery

Ali Moulahi[1], Mohamed Abdefattah Ibrahim[1,2], Issam Mjejri[3], Abdulhadi Hamad Al-Marri[1] and Faouzi Sediri[3,*]

[1]Department of Chemistry, Al-Wajha University College, Tabuk, Saudi Arabia
[2]Department of Chemistry, Faculty of Science in El-Arish, El-Arish University, North Sinai, Egypt
[3]Materials and Environment Research Unit (UR15ES01), IPEIT, University of Tunis, Rue Jawaher Lel Nahru, 1089 Montfleury, Tunisia

Article Type: Article

Article Citation: Ali Moulahi, Mohamed Abdefattah Ibrahim, Issam Mjejri, Abdulhadi Hamad Al-Marri, Faouzi Sediri. Controlled hydrothermal synthesis of nano-MoO_2 as anode for lithium ion battery. *Indian Journal of Science and Technology*. 2020; 13(03), 277-285. DOI: 10.17485/ijst/2020/v013i03/149476

Received date: December 7, 2019

Accepted date: December 30, 2019

***Author for correspondence:**
Faouzi Sediri sediri68@gmail.com
Materials and Environment Research Unit (UR15ES01), IPEIT, University of Tunis, Rue Jawaher Lel Nahru, 1089 Montfleury, Tunisia

Abstract

Objectives/methods: Nano-MoO_2, with different allotropic forms is synthesized through a reduction reaction of molybdenum trioxide in aqueous solutions using ethylene glycol. The structure and morphology characterizations are carried out by XRD, SEM, and Raman. The XRD and SEM data indicate the as-prepared samples present a single and homogeneous phase MoO_2 with monocline symmetry. **Findings/application:** The optical properties of the as-synthesized samples are investigated by photoluminescence. Cyclic voltammetric characterization of MoO_2 films has revealed reversible redox behavior with charge–discharge cycling which corresponds to the reversible lithium intercalation/deintercalation. The electrochemical properties study of the MoO_2 has showed that the monoclinic MoO_2 has a good stability and a nice reversibility, an indicator that the molybdenum dioxide is most suitable for application in lithium-ion batteries (LIBs).

Keywords: Hydrothermal Treatment; Electrode Materials; Electrochemical Properties; Lithium-ion Batteries.

1. Introduction

Transition metal oxides have been widely studied because of its large applications [1–6]. Among these oxides, molybdenum dioxide (MoO_2) shows mainly rich chemistry because of the variable molybdenum oxidation state and its flexible coordination environment [7–8]. Due to their low cost and good electronic conductivity, MoO_2 can also constitute a good electrochemical capacitors and electrode materials for lithium-ion batteries (LIBs) [9–17]. Molybdenum dioxide exists in various polymorphic forms which depend on thermodynamic conditions: hexagonal phase (P63/mmc), tetragonal phase (P42/mnm), and monoclinic phase ($P2_1/n$) [18–20].

Usually, MoO_2 is obtained through a reduction process MoO_3 at a high temperature in the presence of hydrogen [7], but their results exhibited a limited success because only nano-sized powders in zero dimensions were prepared. Hydrothermal treatment involving the reduction of MoO_3 to MoO_2 offers a new approach to synthesis of nano-materials in one, two, or three dimensions under mild conditions, which offers various morphologies and an easy control. In Ref. [21], Zhang et al. have described the synthesis of MoO_2 powders with spheres morphology by a reduction process of the molybdenum trioxide in the presence of diethylenetriamine (DETA). Moreover, Zhang et al. [22] prepared MoO_2 nanosheets via a one-pot solvothermal approach, using an ionic liquid in the reaction system. The authors have studied the electrochemical properties of MoO_2 nanosheets. In fact, this study proves that the MoO_2 can be used as anode materials for Li-ion intercalation because a large reversible capacity, a high rate performance, and a good cycling stability. Obviously, the electrochemical performance of molybdenum dioxide depends on several parameters, including the morphology, the deposition method, the film thickness, the electrolytic medium, and the scan rate. In [23] this study, we expect the same behavior but and in besides these parameters, we studied also the effect on the morphologies of the MoO_2 and the influence of the allotropic forms on the electroactivity of the molybdenum dioxide.

In this study, we described an easy and a low-cost hydrothermal treatment for the synthesis of MoO_2 nanostructured by using MoO_3, as a molybdenum source, and ethylene glycol ($C_2H_6O_2$), as a reducing and structure-directing agent. By varying the synthesis temperature, duration and molar ration a structural change of the MoO_2 phase is observed. The electrochemical properties of the MoO_2 have been investigated using cyclic voltammetry (CV) in the presence of Li^+ in propylene carbonate electrolytic. The influence of the morphology and the allotropic forms of the MoO_2 is discussed. Despite the diversity of synthetic methods of the MoO_2 phase, our study presents a new strategy to get the phase MoO_2 while controlling the morphology and the allotropic form of the MoO_2 phase.

2. Materials and Methods

2.1. Hydrothermal Synthesis

Nano-MoO_2 particles were synthesized through hydrothermal method. All the chemical reagents were purchased from Acros Organics and used without further purification. Molybdenum (+VI) oxide (MoO_3) was used as molybdenum source; ethylene glycol has been used as template. In a typical synthesis, the preparation was made from a mixture of MoO_3, ethylene glycol, and distilled water (5 mL) in a molar ratio of 1:1:385. Reactants were introduced in this order and stirred for a few minutes before introducing the resulting suspension in a Teflon-lined steel autoclave and the temperature set for 4 days at different temperatures. The pH of the solution keeps close to pH = 7 during the whole synthesis. To remove organics residues, the obtained powder was washed with ethanol. It was then dried at 80 °C to lead to a black powder, which suggests that Mo^{6+} ions have been totally reduced to Mo^{4+} through the decomposition of the organic compound.

2.2. Characterization Techniques

The black powders structure was characterized by X-ray diffraction analysis (Philips PW 1820, Instrument, 2θ ranging from 20 to 60° and $\lambda_{CuK\alpha 1}$ = 1.54056 Å). Scanning electron microscopy (SEM) images were recorded with a SEI instrument (operating at 5 kV) microscope. Raman spectroscopy was performed using a Jobin Yvon T 64 000 spectrometer (blue laser excitation with 488 nm wavelength and <55 mW power at the sample). To investigate the optical properties of the samples, photoluminescence (PL) spectroscopy was performed using a 250 mm Jobin Yvon luminescence spectrometer.

2.3. Electrochemical Measurements

The electrodes were fabricated by blending MoO_2 with acetylene black carbon as conductive additive and polyvinylidene difluoride (PVDF), in a weight ratio of 8/1/1, respectively. Homogenous, thick slurry was prepared using N-methylpyrrolidone (NMP) as solvent for the mixture. The slurry was cast on a Cu metal foil and dried in vacuum oven for 12 h at 90 °C. The coin-type cells CR2032 were assembled using the as-prepared electrode as the work electrode; a layer of metallic lithium pasted on the stainless steel disk was used as counter as well as reference electrode. The electrolyte consists of 1 M $LiPF_6$ in mixed ethylene carbonate (EC) and diethyl carbonate (DEC) (the volume ratio of EC to DEC is 1:1). Cyclic voltammetry (CV) experiments were performed in the voltage range of 3.0–0.0 V vs Li/Li^+ using a Biologic VMP-3 model. The electrochemical charge–discharge tests were evaluated at various current rates in a voltage cut off of 3.0 and 0.0 V vs Li/Li^+.

3. Results and Discussion

The first study deals with the composition, structural characterization and the structural transformation of the black powders obtained by the hydrothermal method in the presence of ethylene glycol were determined by X-ray powder diffraction (XRD). The phase of the resulting products obtained from the reducing of the MoO_3 by ethylene glycol at 180 °C for different durations (1 day, 2 and 4 days), as shown in Figure 1. It is noted that the crystalline phases for molybdenum oxide are discriminatory at different reaction times. Indeed, after one and two days of synthesis process (Figure 1a and b), the diffraction pattern shows the presence of the monoclinic MoO_2 (JCPDS data file 00-032-0671, $P2_1/n$ space group) with lattice parameters a = 0.5606 nm, b = 0.4859 nm, and c = 0.5537 nm. When the reaction time is increased to 4 days (Figure 1c), we notice that there is a structural change and that the all diffraction peaks can perfectly indexed to the hexagonal MoO_2 crystalline phase with a = 0.2838 nm and c = 0.4720 nm, according to JCPDS# 50-0739, P63/mmc space group. No peaks of any other phases or impurities were observed from the XRD patterns, indicating that the monoclinic and hexagonal molybdenum dioxide crystalline phase with high purity could be obtained using the present synthetic process. This study demonstrates the impact of the hydrothermal reaction time on the crystalline and structure transformation of the molybdenum dioxide.

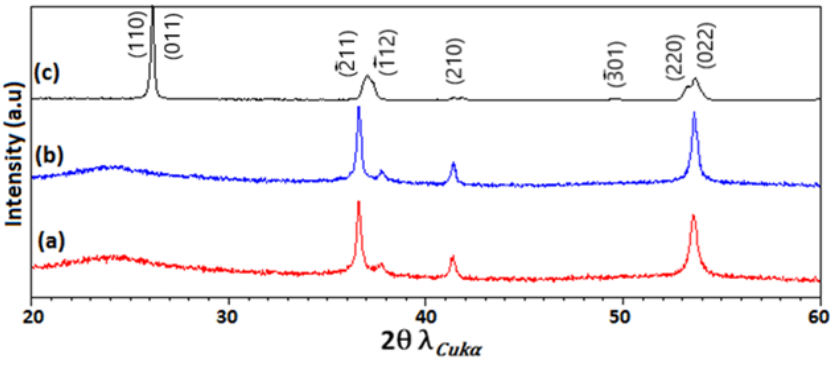

FIGURE 1. Powder X-ray diffraction patterns of the black powders synthesized at 180 °C for (a) 1 day, (b) 2 days, and (c) 4 days.

Various experiments were performed to investigate the effect of modifications to the hydrothermal treatment on the structure and the morphology of the final product. The samples were prepared at different temperatures (140 °C, 180 °C, and 220 °C). At 140 °C (Figure 2a), the diffraction pattern shows the presence of monoclinic MoO_2 (m-MoO_2) (JCPDS data file 00-032-0671, $P2_1/n$ space group). When the temperature increases from 140 to 180 and 220 °C (Figure 2b and c), we notice the disappearance of the peaks characteristic of the monoclinic form and the appearance of the new peaks of high intensity, which are perfectly indexed to the hexagonal MoO_2 (h-MoO_2).

In the remainder of this study, we will be studying the optical and electrochemical properties of two different allotropic forms of the MoO_2 phase (the hexagonal h-MoO_2 phase and the monoclinic m-MoO_2one) synthesized for 4 days at 140 °C, 180 °C, and 220 °C.

The morphology of synthesized materials was studied using the SEM. Figure 3 shows SEM images of the powder (m-MoO_2 and h-MoO_2) synthesized through a hydrothermal method. Monoclinic m-MoO_2 exhibited a hierarchical and homogenous phases with

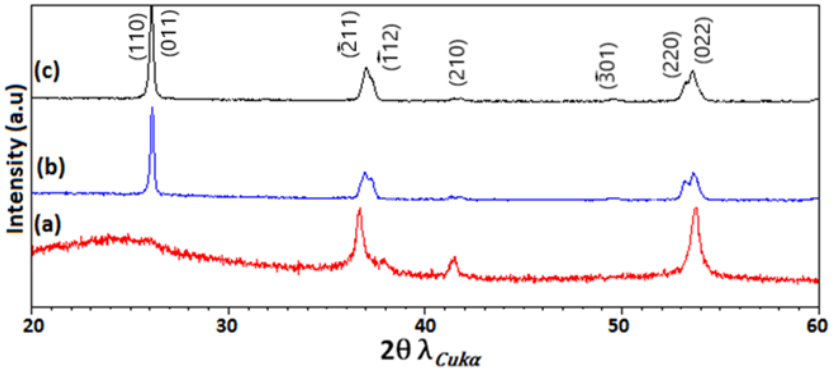

FIGURE 2. Powder X-ray diffraction patterns of the black powders synthesized at 4 days for (a) 140 °C, (b) 180 °C, and (c) 220 °C.

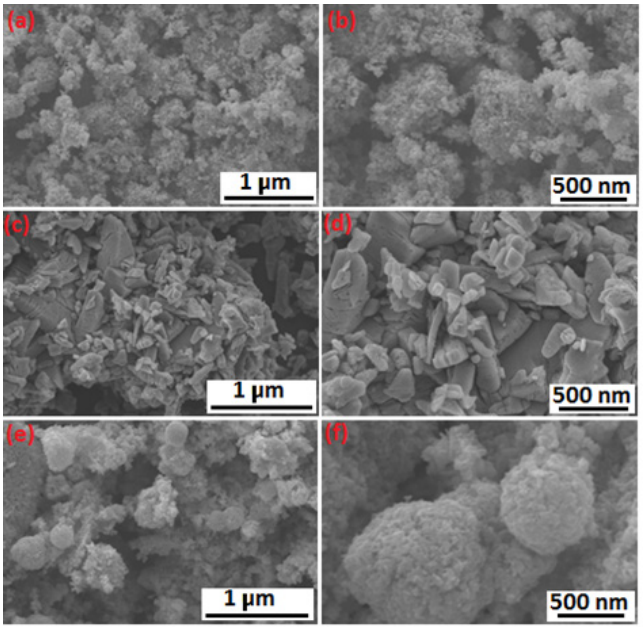

FIGURE 3. SEM of the MoO2 powders synthesized for 4 days at (a, b) 140 °C, (c, d) 180 °C, and (e, f) 220 °C.

isotropic crystallite shapes (Figure 3a and b). From the hexagonal phase synthesized at 180 °C (Figure 3c and d), we notice the presence of irregular particles with irregular size, whereas uniform nanospheres were observed (Figure 3e and f) for product obtained after the lapse of 4 days at 220 °C. The hexagonal MoO_2, synthesized at 220 °C, SEM images show a homogenous phase with uniform nanospheres. These results corroborate that the temperature has a pivotal effect on molybdenum nanomaterials structure and morphology.

The structure of MoO_2 nanoparticles was even more characterized by Raman spectroscopy. A typical room temperature Raman spectroscopy of the m-MoO_2 synthesized at 140 °C and h-MoO_2 synthesized at 180 and 220 °C shown in Figure 4. The monoclinic phase (m-MoO_2) indicates the presence of two intense peaks located at 817 cm^{-1} (Ag, y_s mode) and 990 cm^{-1} (Ag, y_{as} mode) which are assigned to the stretching mode of M=O. From the h-MoO_2, many characteristic peaks are observed, representing O=M=O wagging (290 cm^{-1}), O–M–O bend (340 cm^{-1}), O–M–O stretch (670 cm^{-1}), M=O stretch (817 cm^{-1}, A_g, υ_s) and M=O (990 cm^{-1}, A_g, υ_{as}) stretch, respectively.

The photoluminescence spectra of m-MoO_2 and h-MoO_2 are shown in Figure 5. The three samples exhibit strong PL intensity at about 350 nm, which means a prompt recombination of electrons in the conduction band and holes in the valence band.

To evaluate the stability and the electrochemical performances of the h-MoO_2 as electrode material in batteries lithium ion, cyclic voltammetry analysis was conducted. Figure 6a shows the CVs curves of h-MoO_2 between 0.0 and 3.0 V at 0.1 mV s^{-1}. One reduction peak (0.7 V) and two oxidation peaks (1.3 V and 1.7 V) were observed in the first cycle. The charge measured for reduction process is equal to the charge measured for oxidation (Q_{ox}/Q_{red} = 99%) (shown in Figure 6b). This indicates that all the Li^+ cation

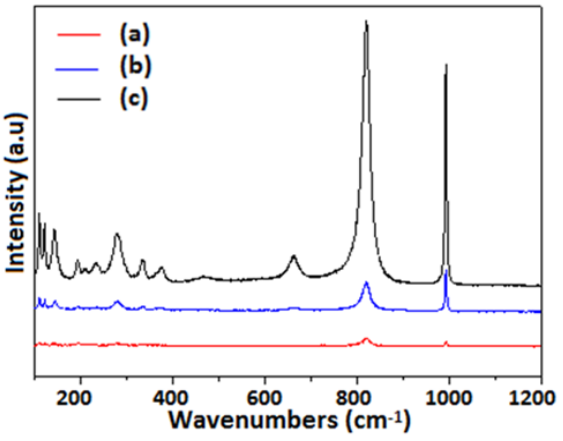

FIGURE 4. Raman spectra of the MoO2 powders synthesized for 4 days at (a) 140 °C, (b) 180 °C, and (c) 220 °C.

inserted in the h-MoO_2 electrode during the reduction process are totally expelled after material oxidation and that the Li^+ intercalation/de-intercalation is totally reversible at 0.1 mV/s scan rate. Figure 5c shows the charge–discharge curves of the h-MoO_2 for the first and second cycles at a current density of 100 mA g^{-1}. It can be found that the material display the discharge and charge capacities of 345 mAh g^{-1} and 250 mAh g^{-1}, respectively at the first cycle. As for the second cycle, the discharge and charge capacities of h-MoO_2 are 250 and 248 mAh g^{-1}. The initial capacities loss of 95 mAh g^{-1} due to the formation of solid electrolyte interface (SEI) layer. Figure 6d shows the cycling performances of the h-MoO_2 electrode. As expected, under the rate of 100 mA g^{-1}, the h-MoO_2 electrode shows a high discharge capacity (360 mAh g^{-1}) and maintains 255 mAh g^{-1} after 50 cycles. The electrochemical performance of the h-MoO_2 nanoparticle is attributed to the nanospheres structure with small diameter and efficient one-dimensional electron transport pathways.

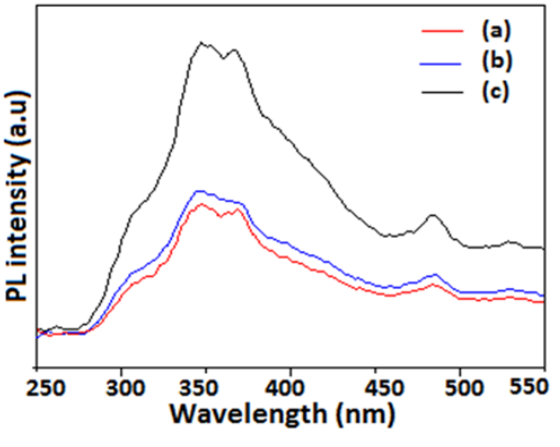

FIGURE 5. Photoluminescence spectra of the MoO2 powders synthesized for 4 days at (a) 140 °C, (b) 180 °C, and (c) 220 °C.

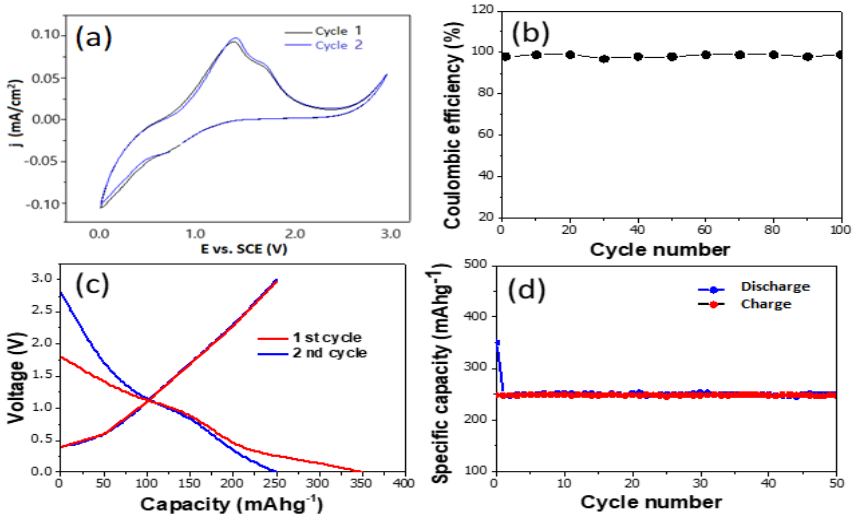

FIGURE 6. (a) CV curves of h-MoO2 electrode; (b) Columbic efficiency of h-MoO2 electrode (c) charge/discharge voltage profiles of h-MoO2 at a current density of 0.1 A g−1, and (d) the specific capacity of the h-MoO2.

4. Conclusion

We have successfully controlled synthesized m-MoO_2 and h-MoO_2 via an easy hydrothermal way from the mixture of MoO_3 and ethylene glycol under soft conditions. The hydrothermal conditions, as duration and temperature, played an important role in the structure and the morphology of the final product. The h-MoO_2 electrode demonstrated (a) high reversible capacity, (b) excellent cycling performance, and (c) good rate capacity as an anode electrode material for Li-ion batteries.

Conflicts of Interest

The authors declare no conflict of interest.

Acknowledgement

This activity included in the project number S-0040-1440 has received funding from the University of Tabuk.

The author would like to acknowledge the University of Tabuk for the financial support under research project number S-0040-1440 and Mr. Tarek Fezai for proofreading and editing the English version.

References

1. Poizot P, Laruelle S, Grugeon S, Dupont L, Tarascon JM. Nano-sized transition-metal oxides as negative-electrode materials for lithium-ion batteries. Nature. 2000; 407, 496–499. DOI: 10.1038/35035045.
2. Ku JH, Jung YS, Lee KT, Kim CH, Oh SM. Thermo electrochemically activated MoO_2 powder electrode for lithium secondary batteries. Journal of the Electrochemical Society. 2009; 156, A688–A693. DOI: 10.1149/1.3141670.
3. Nguyen TD, Do TO. Solvo-hydrothermal approach for the shape-selective synthesis of vanadium oxide nanocrystals and their characterization. Langmuir. 2009; 25(9), 5322–5332. DOI: 10.1021/la804073a.
4. Quiroz HP, Dussan A. Synthesis temperature dependence on magnetic properties of cobalt doped TiO2 thin films for spintronic applications. Applied Surface Science. 2019; 484, 688–691. DOI: 10.1016/j.apsusc.2019.03.068.
5. Zhu M, Meng W, Huang Y, Huang Y, Zhi C. Proton-insertion-enhanced pseudocapacitance based on the assembly structure of tungsten oxide. ACS Applied Materials & Interfaces. 2014; 6(1), 18901–18910. DOI: 10.1021/am504756u.
6. Ahmed B, Shahid M, Nagaraju DH, Anjum DH, Hedhili MN, Alshareef HN. Surface passivation of MoO3 nanorods by atomic layer deposition toward high rate durable Li ion battery anodes. ACS Applied Materials & Interfaces. 2015; 7(24), 13154–13163. DOI: 10.1021/acsami.5b03395.
7. Hu B, Mai L, Chen W, Yan F. From MoO_3 nanobelts to MoO_2 nanorods: structure transformation and electrical transport. ACS Nano. 2009; 3(2), 478–482. DOI: 10.1021/nn800844h.
8. Lüdtke T, Wiedemann D, Efthimiopoulos I, Becker N, Seidel S, Janka O, Pöttgen R, Dronskowski R, Müller MK, Lerch M. HP-MoO_2: a high-pressure polymorph of molybdenum dioxide. Inorganic Chemistry. 2017; 56(6), 2321–2327. DOI: 10.1021/acs.inorgchem.6b03067.
9. Liu Y, Zhang H, Ouyang P, Li Z. One-pot hydrothermal synthesized MoO2 with high reversible capacity for anode application in lithium ion battery. Electrochimica Acta. 2013; 102, 429–435. DOI: 10.1016/j.electacta.2013.03.195.
10. Liang Y, Yi Z, Yang S, Zhou L, Sun J, Zhou Y. Hydrothermal synthesis and lithium-intercalation properties of MoO2 nano-particles with different morphologies. Solid State Ionics. 2006; 177(5–6), 501–505. DOI: 10.1016/j.ssi.2005.12.001.
11. Petnikota S, Teo KW, Chen L, Sim A, Marka SK, Reddy MV, Srikanth VVS, Adams S, Chowdari BVR. Exfoliated graphene oxide/ MoO_2 composites as anode materials in lithium-ion batteries: an insight into intercalation of Li and conversion mechanism of MoO_2. ACS Applied Materials & Interfaces. 2016; 8(17), 10884–10896. DOI: 10.1021/acsami.6b02049.
12. Guo B, Fang X, Li B, Shi Y, Ouyang C, Hu YS, Wang Z, Stucky GD, Chen L. Synthesis and lithium storage mechanism of ultrafine MoO_2 nanorods. Chemistry of Materials. 2012; 24, 457–463. DOI: 10.1021/cm202459r.
13. Xu Z, Wang H, Li Z, Kohandehghan A, Ding J, Chen J, Cui K, Mitlin D. Sulfur refines MoO_2 distribution enabling improved lithium ion battery performance. The Journal of Physical Chemistry C. 2014; 118(32), 18387–18396. DOI: 10.1021/jp504721y.
14. Bhaskar A, Deepa M, Rao TN. MoO_2/multiwalled carbon nanotubes (MWCNT) hybrid for use as a Li-ion battery anode. ACS Applied Materials & Interfaces. 2013; 5(7), 2555–2566. DOI: 10.1021/am3031536.
15. Shi YF, Guo BK, Corr SA, Shi QH, Hu YS, Heier KR, Chen LQ, Seshadri R, Stucky GD. Ordered mesoporous metallic MoO2 materials with highly reversible lithium storage capacity. Nano Letters. 2009; 9(12), 4215–4220. DOI: 10.1021/nl902423a.

16. Sun YM, Hu XL, Luo W, Huang YH. Self-assembled hierarchical MoO2/graphene nanoarchitectures and their application as a high-performance anode material for lithium-ion batteries. ACS Nano. 2011; 5, 7100–7107. DOI: 10.1021/nn201802c.
17. Fleischmann S, Zeiger M, Quade A, Kruth A, Presser V. Atomic layer-deposited molybdenum oxide/carbon nanotube hybrid electrodes: the influence of crystal structure on lithium-ion capacitor performance. ACS Applied Materials & Interfaces. 2018; 10(22), 18675–18684. DOI: 10.1021/acsami.8b03233.
18. Nishanthi ST, Baruah A, Yadav KK, Sarkerbe D, Ghosh S, Ganguliac AK, Jha M. New low temperature environmental friendly process for the synthesis of tetragonal MoO_2 and its field emission properties. Applied Surface Science. 2019; 467–468, 1148–1156. DOI: 10.1016/j.apsusc.2018.10.173.
19. Alves LMS, Oliveira FS, de Lima BS, da Luz MS, Rebello A, Masunaga SH, Neumeier JJ, Gilesde C, Leão JB, dos Santos CAM. Evidence of phase transitions in MoO_2 single crystals. Journal of Alloys and Compounds. 2017; 705, 764–768. DOI: 10.1016/j.jallcom.2017.02.148.
20. Becker N, Dronskowski R. A first-principles study on new high-pressure metastable polymorphs of MoO2. Journal of Solid State Chemistry. 2016; 237, 404–410. DOI: 10.1016/j.jssc.2016.03.002.
21. Zhang H, Li Y, Hong Z, Wei M. Fabrication of hierarchical hollow MoO_2 microspheres constructed from small spheres. Materials Letter. 2012; 79, 148–151. DOI: 10.1016/j.matlet.2012.03.105.
22. Zhang H, Zeng L, Wu, X, Lian L, Wei M. Synthesis of MoO_2 nanosheets by an ionic liquid route and its electrochemical properties. Journal of Alloys and Compounds. 2013; 580, 358–362. DOI: 10.1016/j.jallcom.2013.06.100.
23. Li X, Xiao Q, Zhang H, Xu H, Zhang Y. Fabrication and application of hierarchical mesoporous MoO2/Mo2C/C microspheres. Journal of Energy Chemistry. 2018; 27(3), 940–948. DOI: 10.1016/j.jechem.2017.09.008.